ROYAL SOCIETY OF CHEMISTRY

Check for updates

Fully biobased and biodegradable oxygen barrier coating for poly(lactic acid)†

Sarah G. Fisher,[a] Armaghan Amanipour,[b] Maya D. Montemayor,[a] Ethan T. Iverson,[a] Edward Chang,[c] Alexandra V. Moran,[c] Reza Ovissipour[b] and Jaime C. Grunlan [ID] *[acd]

Concerns regarding single-use petroleum-based plastic have led to a push toward bioplastic packaging. Poly(lactic acid) (PLA), one of the most utilized bioplastics, suffers from poor oxygen barrier that limits its application as a packaging material. In this work, layer-by-layer nanocoatings consisting of chitosan, deoxyribonucleic acid (DNA), and cellulose nanocrystals are applied to PLA to improve its barrier performance. These coatings decrease the oxygen transmission rate of PLA by up to 30× at just 120 nm of thickness, placing them among the best-performing fully biobased barriers ever reported. Combinations of coating materials are investigated to provide the best performance in both dry and humid conditions. The effect of humidity on the barrier performance is found to depend heavily on the presence of cellulose nanocrystals in the film. Additionally, the biobased coatings do not impede the biodegradability of the PLA substrate. The barrier technology and deposition process fulfill the principles of green chemistry and represent a significant improvement in sustainable gas barrier films.

Sustainability spotlight

Poly(lactic acid) (PLA) is a promising alternative to conventional petroleum-derived plastics. It has a much lower carbon footprint and is both bioderived and biodegradable. Despite its promise, the use of PLA for food packaging is limited by its poor oxygen barrier. In this study, barrier coatings are developed for PLA using only biobased materials. The coating deposition process is water-based and performed under ambient conditions. The coatings do not impede the biodegradability of the PLA. Furthermore, the barrier performance achieved is among the best reported for a biobased oxygen barrier coating. This work contributes to the UN sustainable development goals of industry, innovation, and infrastructure (SDG 9) and responsible consumption and production (SDG 12).

Introduction

Plastic waste is accumulating on our planet at an alarming rate. About 80% of plastic ends up in landfills and the natural environment after use, and petroleum-based polymers take thousands of years to degrade.[1,2] Plastic packaging makes up the largest portion of global plastic consumption (>30%).[1] There is growing interest in shifting to the use of bioplastics for packaging applications.[3] Poly(lactic acid), or PLA, is a commonly used bioplastic synthesized from lactic acid, which is derived from

[a]Department of Chemistry, Texas A&M University, 400 Bizzell St, College Station, TX, 77840, USA. E-mail: jgrunlan@tamu.edu

[b]Department of Food Science and Technology, Texas A&M University, 400 Bizzell St, College Station, TX, 77840, USA

[c]Department of Mechanical Engineering, Texas A&M University, 400 Bizzell St, College Station, TX, 77840, USA

[d]Department of Materials Science and Engineering, Texas A&M University, 400 Bizzell St, College Station, TX, 77840, USA

† Electronic supplementary information (ESI) available: Description of CNC characterization; AFM images of CNCs; measured and reported dimensions of CNCs; optical images and visible light transmission of uncoated and coated PLA; coating thickness, OTR, and oxygen permeability values; AFM images of LbL coatings. See DOI: https://doi.org/10.1039/d4su00714j

biomass.[2,3] PLA is industrially processable, has a significantly lower carbon footprint than conventional plastics, and is biodegradable.[2,4,5] Despite these benefits, the use of PLA is limited by its poor barrier properties.[2,4] Oxygen barrier performance is particularly important for food packaging to prevent contamination and degradation leading to food waste.[2,6]

Typical approaches to improve the oxygen barrier of PLA include lamination with petroleum-based plastics, vacuum deposition of metal oxides, or forming nanocomposites with clay or other nanoparticles. These approaches provide limited improvements and/or impede desirable properties such as transparency and biodegradability.[1,7–9] Another technique to improve barrier performance is layer-by-layer (LbL) assembly, which utilizes electrostatic interactions between complementary materials (*e.g.*, polyelectrolytes and nanoparticles) to deposit multilayer films.[8,10,11] LbL films are typically prepared by sequentially immersing a charged substrate into aqueous solutions containing materials of alternating charge to form repeating layers of oppositely charged materials.[11] These multilayer films can have very low oxygen permeabilities due to their dense, ionically-crosslinked structure, high cohesive energy, and high degree of nanofiller orientation perpendicular to the direction of permeant diffusion. Although most of the

reported LbL gas barrier coatings utilize synthetic and nonrenewable polymers and nanomaterials, the LbL coating technique can also be utilized with biomaterials.

Chitosan (CH) and cellulose nanocrystals (CNCs) are two of the most widely utilized biomaterials in barrier film technology.[6,12–15] CH, a cationic polyelectrolyte primarily obtained from shellfish waste, has been widely used in LbL assembly for gas barrier coatings.[12,14,16] CNCs, which are extracted from cellulosic biomass, are stiff, rod-like, highly crystalline materials.[17] They are commonly incorporated as fillers in barrier packaging due to their inherently low oxygen permeability and their capacity to form a highly tortuous pathway for permeant molecules inside a polymer matrix.[4,17,18] CNCs have been utilized in LbL barrier films with other biomaterials, including chitosan.[14,19] In contrast to CH and CNCs, deoxyribonucleic acid (DNA) has not been studied broadly for barrier applications. Valle *et al.* recently published the first DNA-containing LbL film for gas barrier applications.[16] This film, which was constructed of CH and DNA, decreased the oxygen permeability of the substrate by about 2× at 0% relative humidity, but the barrier was not retained at high humidity.

In this work, LbL coatings consisting of CH, CNCs, and DNA are evaluated for their ability to improve the oxygen barrier of a PLA substrate at low and high humidity. These optically transparent films decrease the oxygen permeability of PLA by 6 to 30× at ~100 nm thickness, placing them among the best-performing biobased barriers ever reported. The water sensitivity of the films is found to be tunable based on the incorporation of CNCs. Furthermore, these coatings do not impede the biodegradability of the PLA substrate. This work represents a significant improvement to the oxygen barrier of PLA without hindering its desirable attributes as a biobased and biodegradable packaging material.

Experimental

Materials and solution preparation

Deoxyribonucleic acid from herring sperm (<50 bp, degraded), glacial acetic acid, hydrochloric acid (HCl, ACS reagent, 37%), and sodium hydroxide (NaOH, ACS reagent, pellets) were purchased from Sigma-Aldrich (Milwaukee, WI, USA). DNA was stored at 7 °C until use. Chitosan (95% deacetylated) was purchased from Greentech Biochemicals (Qingdao, China). Cellulose nanocrystals (CelluForce NCC® NCV100-NASD90) were purchased from CelluForce (Montreal, Quebec, Canada). Poly(lactic acid) (0.05 mm thick, 330 mm coil, amorphous) was
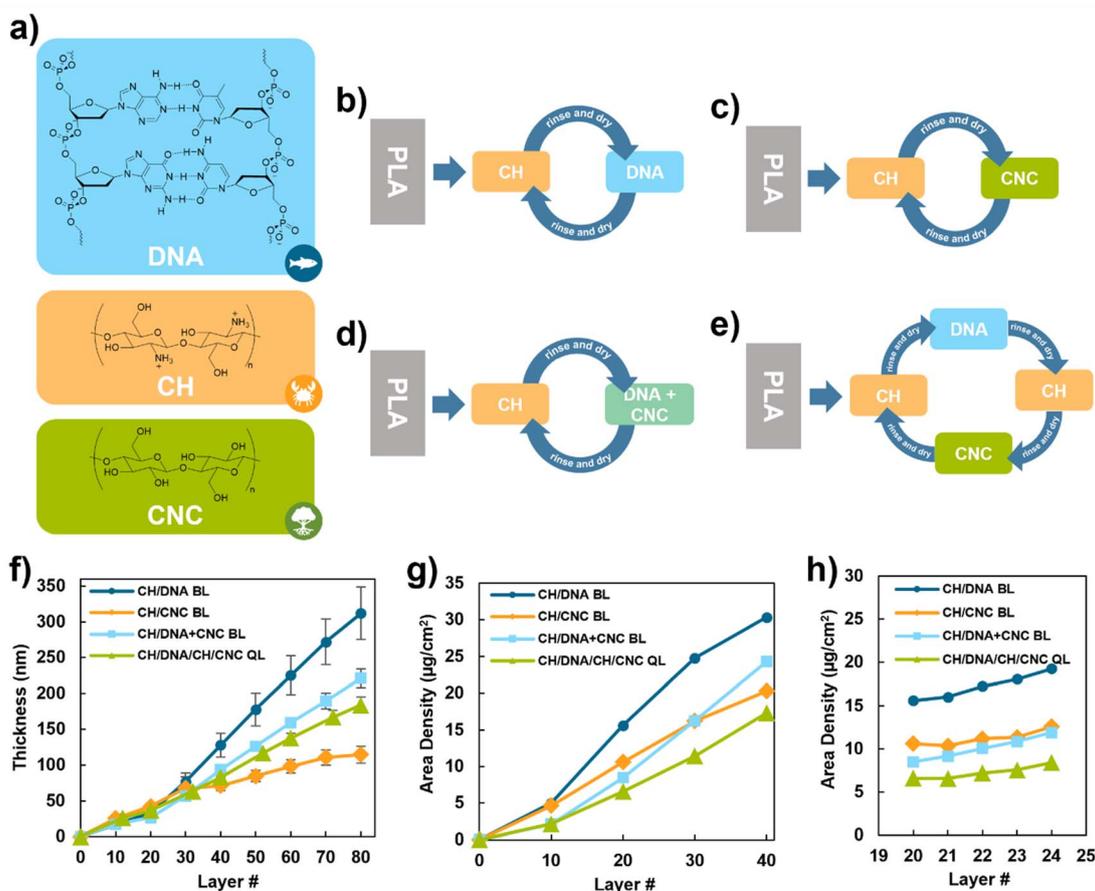

Fig. 1 (a) Chemical structures of coating components. Layer-by-layer schematics of coating systems: (b) CH/DNA BL, (c) CH/CNC BL, (d) CH/DNA + CNC BL, and (e) CH/DNA/CH/CNC QL. (f) Thickness and (g and h) area density of layer-by-layer coatings as a function of layer number. Error bars are too small to be observed in (g) and (h).

purchased from Goodfellow (Coraopolis, PA, USA) and used as the substrate for oxygen transmission rate testing, water contact angle experiments, scanning electron microscopy, optical images, UV-vis spectroscopy, and biodegradation experiments. Single-side polished, 500 μm-thick Si wafers were purchased from University Wafer (South Boston, MA, USA) and used as substrates for thickness measurements, atomic force microscopy, and ellipsometry swelling tests. 18 MΩ deionized (DI) water was used to prepare all solutions and for all rinsing procedures. CH solutions were prepared by dissolving 0.2 wt% CH in 0.25 M acetic acid. DNA solutions were prepared by dissolving 0.2 wt% DNA in DI water. CNC solutions were prepared by dispersing 1 wt% CNC in DI water. For solutions containing both DNA and CNC, equal volumes of 0.4 wt% DNA and 2 wt% CNC solutions were combined to result in a solution that was 0.2 wt% DNA and 1 wt% CNC. All solutions were adjusted to pH 4 using 5 M HCl and 5 M NaOH. After adjusting the pH, solutions were stirred for 1 hour before the pH was re-adjusted to 4 as needed. Solutions were utilized immediately after the second pH adjustment. The chemical structures of DNA, CH, and CNC are depicted in Fig. 1a.

Film fabrication

Immediately before coating, substrates were rinsed with DI water, methanol, then DI water again, dried with compressed air, and plasma treated for five minutes to improve coating adhesion. The coating procedure for each system is summarized in Fig. 1. For the three bilayer (BL) systems (Fig. 1b–d), the treated substrate was immersed in the CH solution for 5 minutes, then rinsed with DI water and dried with compressed air. The substrate was then immersed in the subsequent solution (DNA, CNC, or DNA + CNC) for 5 minutes, rinsed with DI water, and dried with compressed air to complete the first BL. Subsequent BLs proceeded as described for the first BL, but the dip time was shortened to 1 minute. For the quadlayer (QL) system (Fig. 1e), the treated substrate was immersed in the CH solution for 5 minutes, then rinsed with DI water and dried with compressed air. The substrate was then immersed in the DNA solution for 5 minutes, rinsed with DI water, and dried with compressed air. Next the substrate was immersed in a second CH solution for 1 minute, rinsed with DI water, and dried with compressed air. The substrate was then immersed in the CNC solution for 1 minute, rinsed with DI water, and dried with compressed air to complete the first QL. Subsequent QLs proceeded as described for the first QL, but the dip time was shortened to 1 minute for all layers.

Characterization

A Bruker Dimension Icon atomic force microscope [AFM] (Billerica, MA, USA) was used to evaluate the dimensions of the CNCs, as well as the surface morphology and roughness of the LbL films. CNC solutions were prepared at 0.005 wt%, drop-cast on plasma treated Si wafers, and dried at 70 °C for 1 hour before analyzing with AFM. Dynamic light scattering (DLS) experiments were performed using a Zetasizer Nano ZS (Malvern, Worcestershire, United Kingdom) on CNC coating solutions

diluted by a factor of 30 and re-adjusted to pH 4. Film thickness was measured in triplicate using a P6 profilometer (KLA-Tencor, Milpitas, CA, USA) or Alpha-SE ellipsometer (J.A. Woollam Co., Lincoln, NE, USA). PLA substrate thickness was measured using a Thwing-Albert ProGage touch thickness tester (West Berlin, NJ, USA). Ten measurements were averaged to determine the substrate thickness. A quartz crystal microbalance [QCM] (Maxtek Inc., Cypress, CA, USA) was utilized to determine the area density (mass per area) of the films at set layer numbers. Visible light transmission of coated and uncoated PLA was measured from 380 to 850 nm using an Ocean Optics USB2000+ spectrometer equipped with a DH-mini light source. The background was established with an uncoated, untreated PLA sample. Static water contact angles were measured using a KSV CAM 200 instrument (KSV Instruments, Ltd, Monroe, CT, USA). Data was recorded 30 seconds after depositing a 5 μL DI water droplet on the surface of coated or uncoated PLA. 20 datapoints were recorded for each sample. Water swelling behavior was measured using an Alpha-SE ellipsometer equipped with a 500 μL LiquidCell (J.A. Woollam Co., Lincoln, NE, USA). 20 BL or 10 QL films coated on Si wafers were measured in triplicate before filling the cell with water, immediately after adding water to the cell, and 15 minutes after the addition of water. Oxygen transmission rate was measured by Ametek MOCON, Inc. (Minneapolis, MN) using an Oxtran 2/21 instrument in accordance with ASTM D3985 and ASTM F1927. Oxygen was utilized as the test gas at 23 °C, with a relative humidity (RH) of 0% and 90%. Oxygen permeability values of the LbL films were calculated from OTR, thickness, and oxygen partial pressure in accordance with ASTM D3985 and F1927.

Biodegradation

Enzymatic hydrolysis of coated and uncoated PLA samples was performed using a method described by Valle *et al.* with slight modifications.[16] Uncoated and coated PLA film disks (5 mm in diameter, $n = 3$) were placed individually in a 1.5 mL Eppendorf tube with 1 mL of a 10 μM solution of cutinase enzyme Novozym® 51032 (Strem Chemicals, Newburyport, MA, USA) in 0.1 M phosphate buffer solution at pH 8 (Reagents, North Carolina, USA). Samples were incubated for 24, 72, 120, and 168 hours at 50 °C and 100 rpm in an INNOVA 4300 shaker incubator (New Brunswick Scientific Co., Inc., Edison, NJ, USA) to ensure effective exposure of films to the enzyme solution. At each time point, the samples were removed from the tubes, washed three times with Mili-Q water and then dried at 30 °C overnight. The weight of each film was measured using an analytical balance. The pH of the solution after film removal was also measured at each time point.

Results and discussion

Film growth

The growth profiles of the films are shown in Fig. 1f. The CH/DNA and CH/DNA + CNC BL films exhibit superlinear growth, whereas the CH/CNC BL and CH/DNA/CH/CNC QL films exhibit linear growth, reaching lower thicknesses at the same number

of layers. The transition in growth rate, which occurs around 20 layers for the CH/DNA and CH/DNA + CNC systems, can be attributed to a transition from island growth deposition to chain interpenetration.[10] The CH/DNA films are understood to grow thickest due to uninhibited interpolymer interactions, leading to polymer interdiffusion and charge overcompensation in a typical "in-and-out" mechanism of all-polymer LbL film growth.[20,21] The presence of nanomaterials, on the other hand, is expected to hinder growth, as the CNCs create barriers to polymer diffusion.[22,23] It is apparent from Fig. 1f that films containing more CNC layers grow thinner, with the CH/CNC films growing to only ~115 nm at 80 layers (40 BL). The QL film, which has half as many CNC-only layers as the CH/CNC film, grows significantly thicker, achieving ~185 nm at 80 layers (20 QL). The CH/DNA + CNC film has no CNC-only layers, and as a result thicker growth (~220 nm at 80 layers) is achieved through polymer–polymer interpenetration.

It should be noted that the presence of CNCs still limits the film growth relative to the polymer-only film, which grows to ~315 nm at 80 layers. This is further supported with quartz crystal microbalance (QCM) experiments, where the CH/DNA film achieves the highest area density at 40 layers, and the CH/DNA + CNC exhibits the second highest value (Fig. 1g). The CH/CNC and CH/DNA/CH/CNC films have similar area density values at 40 layers, which is consistent with their similar thickness values at that layer number (Fig. 1f). Individual layer deposition was also analyzed with QCM (Fig. 1h). For the CH/DNA and CH/DNA + CNC systems, the area density increases steadily with each layer. In contrast, the CH/CNC and QL films show decreases in area density in the layers that follow CNC-only layers. This is attributed to relatively weak adhesion of CNCs to the preceding CH layer, resulting in some rinsing off in the subsequent dipping step. It is believed that this does not occur with the CH/DNA + CNC film because the DNA polymer entraps the CNCs, aiding in their adhesion to the film's surface. It has been observed that combining a polyelectrolyte with a nanomaterial in a bilayer system results in better nanomaterial alignment and incorporation.[24] All of the films exhibit high transparency at 40 layers (20 BL or 10 QL), with visible light transmission over 90% relative to an untreated PLA substrate (Fig. S2†). This high transparency is typical for LbL films and confirms that the CNC nanoparticles are generally well separated and aligned within the films.[25]

Oxygen barrier

Films for oxygen barrier testing were grown to 20 BL or 10 QL (40 total layers) and tested at low (0%) and high (90%) relative humidity (RH). At 0% RH, all films exhibit a substantial improvement in barrier when compared to the PLA substrate (Fig. 2a). Untreated and plasma treated PLA have similar oxygen transmission rates (OTRs) of 323 and 331 cm^3 per m^2 per day, respectively (Table S2†). At 0% RH, the best-performing barrier coating is the QL film, with an OTR of 10.9 cm^3 per m^2 per day, resulting in a ~30× improvement over uncoated PLA. The CH/DNA + CNC film exhibits a similarly low OTR of 12.0 cm^3 per m^2 per day, while the CH/DNA film has a slightly higher OTR of 15.1
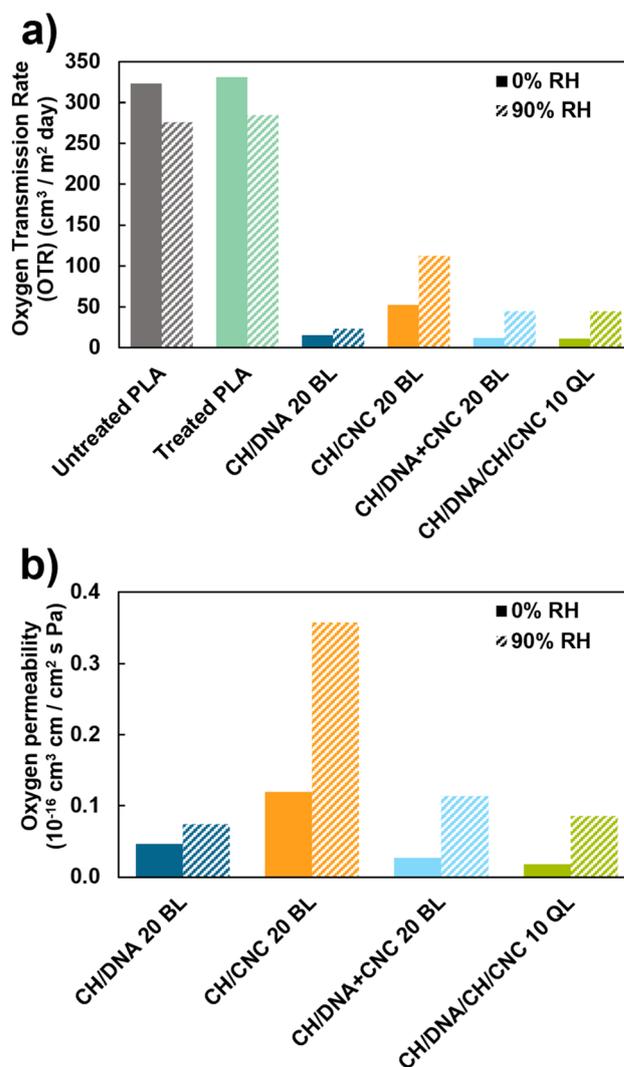

Fig. 2 (a) Oxygen transmission rate of coated and uncoated treated PLA at 0% and 90% RH and (b) oxygen permeability of LbL films at 0% and 90% RH. "Treated PLA" refers to uncoated PLA that has been plasma treated.

cm^3 per m^2 per day. The CH/CNC film has the highest OTR of all the coated PLA samples, at 52.6 cm^3 per m^2 per day. This is over 3× higher than the other three systems' OTR values at the same number of layers. The films containing CNC particles were expected to have superior barrier performance due to the highly crystalline CNCs forming a tortuous pathway within the film, forcing oxygen molecules to travel a greater distance around the impenetrable CNCs in order to permeate through the film.[26] It appears that this benefit only occurs when DNA is also present in the film. As discussed previously, the QCM data (Fig. 1h) suggests there is poorer adhesion between CH and CNC than there is between CH and DNA or CH and DNA + CNC. This is seen by the mass loss after CNC dipping steps, which is not observed for DNA or DNA + CNC steps. Poor adhesion between polymer and filler particles can result in void formation, increasing the permeability of a film.[27] It is hypothesized that the presence of DNA improves the adhesion and deposition of

Table 1 Water sensitivity and roughness of LbL films

System	Permeability change with humidity (%)	Water contact angle (°)	% swelling ($t = 15$ min)	Average roughness (nm)
Untreated PLA	−15%	70.0 ± 2.5	—	—
Treated PLA	−14%	69.0 ± 3.1	—	—
CH/DNA 20 BL	+54%	48.9 ± 0.9	60.4	1.1 ± 0.2
CH/CNC 20 BL	+113%	29.7 ± 1.6	125.8	3.8 ± 0.3
CH/DNA + CNC 20 BL	+272%	44.5 ± 1.4	114.3[a]	1.6 ± 0.2
CH/DNA/CH/CNC 10 QL	+307%	23.4 ± 1.1	84.0	3.6 ± 0.2

[a] The thickness of the CH/DNA + CNC 20 BL system was not able to be measured at $t = 15$ min, so the % swelling at $t = 0$ min is listed.

the CNCs, decreasing free volume and potential voids in the film.[24]

Disparities in barrier performance are also supported by the film roughness (Table 1 and Fig. S3†). The CH/CNC film has the highest roughness out of all four systems, and films containing CNC-only layers (CH/CNC and CH/DNA/CH/CNC) have significantly higher roughness than the other two films. This supports the idea of a higher degree of disorder and potential defect sites in CNC-only layers. Furthermore, increased spacing between CNC layers in the QL system can help fill in potential defect sites and improve the barrier by increasing the tortuous path length, as previously reported when there is increased spacing of nanoparticle layers in a LbL film.[23,28]

Humidity effects

Hydrophilic polymers tend to show low gas permeability in dry conditions, but lose this property in humid conditions.[18] When plasticized with water, both polymer chains and penetrant molecules become more mobile, increasing the gas transmission rate of the material.[29] As a result, all four of the LbL systems investigated have higher OTR values at 90% RH compared with 0% RH (Fig. 2a and Table S2†). It should be noted that the change in permeability with high humidity is strongly dependent on the presence of CNCs in the system. The CH/DNA film exhibits a humid OTR of 23.2 cm³ per m² per day (a 54% increase in oxygen permeability from 0% RH). In contrast, the CNC-containing films all have increases in oxygen permeability of over 100% (Table 1). The CH/DNA + CNC and QL films have similar humid OTRs of 44.6 and 44.4 cm³ per m² per day, respectively (or oxygen permeability increases of 272% and 307%, respectively). The CH/CNC films exhibit the highest humid OTR of all at 112 cm³ per m² per day, but the 0% RH OTR of the system is already significantly higher than the other films, so this only represents a 113% increase in OTR from 0% to 90% RH. The poorer performance of the CNC-containing films at high humidity is attributed to the highly hydrophilic nature of CNCs. CNCs are especially hydrophilic due to the large number of hydroxyl groups in the structure, making them very susceptible to humidity-induced swelling and loss of barrier.[30] Although all polyelectrolytes are expected to be sensitive to humidity due to their highly polar nature, CNCs appear to have a greater impact than DNA on the water sensitivity of the film. This finding is supported by the work of Valle and coworkers, who found that the oxygen permeability of a CH/DNA gas

barrier film increased by approximately 90% when the humidity changed from 0% to 90%.[16] In contrast, CNC films have been reported to increase in oxygen permeability by over 900% when relative humidity is increased from 7.7% to 80%.[18] Therefore, it is believed that the moisture sensitivity of the films is more dependent on the presence of CNCs than CH or DNA.

The OTR values of the uncoated (both treated and untreated) PLA substrates decrease slightly as the humidity increases. This phenomenon has been observed previously in amorphous poly(ethylene terephthalate), PLA, and polyamide.[31,32] At high humidity, water molecules reduce the oxygen solubility coefficient of the film by competing with oxygen molecules for a limited number of binding sites within the film. Although the plasticization of PLA increases the free volume, and thus the diffusion coefficient, the decrease in oxygen solubility dominates the oxygen permeability, resulting in a lower OTR at high humidity.[33] Overall, the plasma pretreatment has little influence on the PLA oxygen barrier.

The higher moisture sensitivity of CNC-containing films was confirmed with water contact angle experiments and ellipsometry swelling tests. Table 1 shows the average water contact angle of untreated PLA, plasma-treated PLA, and PLA coated with each of the four LbL systems. All the LbL films have lower contact angles (greater hydrophilicity) than the uncoated PLA due to the highly polar nature of the polyelectrolyte-based coatings. The CH/DNA and CH/DNA + CNC films have similar contact angles of 45 to 50°, respectively. In contrast, the films terminated with a CNC-only layer exhibit the highest hydrophilicity, with contact angles between 20 and 30°. This supports the assertion that CNCs are more hydrophilic than DNA. With that said, contact angle values are likely insufficient to fully understand the hydrophilicity of the films due to these measurements being dependent on film roughness. An increase in roughness is expected to increase the hydrophilic or hydrophobic character of a film by increasing the surface area exposed to the water droplet.[34] Both of the films terminated with CNC-only layers exhibit similar roughness values that are significantly higher than those of the other films (Table 1). Therefore, the significantly lower contact angles measured for these samples may be partially attributed to the influence of surface roughness.

Water swelling tests were also performed to elucidate the relationship between a given LbL system and water sensitivity. Fig. 3 shows the results of these tests. The initial value is the
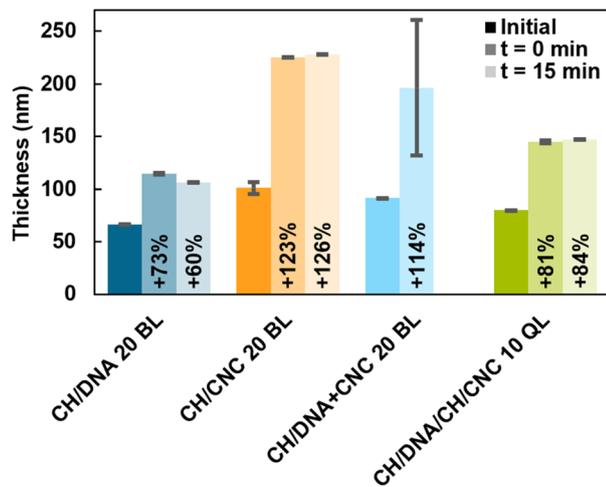
Fig. 3 Thickness of LbL films as a function of water swelling time.

Fig. 4 (a) Mass loss as a function of time and (b) pH of buffer solution as a function of time for coated and uncoated PLA in biodegradability test.

thickness of the film (measured by ellipsometry) before water contact. The $t = 0$ value is the thickness of the film immediately after the ellipsometer cell was filled with deionized water. The $t = 15$ value is the film thickness 15 minutes after filling the cell with water. The CH/DNA system has the lowest water sensitivity, but still swells substantially, increasing its thickness by 60% after 15 minutes of hydration. The CH/DNA + CNC film swells to such a great extent immediately upon contact with water that only two measurements could be taken at $t = 0$ before the film was too swollen to be measurable with ellipsometry. Thickness measurements were impossible after 15 minutes of water contact. Although a precise thickness value could not be obtained at $t = 15$, it can be inferred from this result that the CH/DNA + CNC film is the most susceptible to swelling. The CH/CNC film is also extremely sensitive to water swelling, increasing in thickness by 126% in 15 minutes. The QL film, while more sensitive to water than the CH/DNA film, only swelled by 84% after 15 minutes in water. In contrast, the other two CNC-containing films swelled by over 100% in this time. These results support the hypothesis that CNC-containing films are more sensitive to moisture than CH/DNA films. It is believed that the QL film is less sensitive to swelling than the other CNC-containing films because it has only 10 CNC-containing layers, while the other systems have 20 CNC layers. The water contact angle and swelling data suggest that CNC-containing films exhibit higher sensitivity to moisture and, as a result, more significant barrier loss at high humidity.

Biodegradation

Enzymatic degradation experiments were performed to confirm that coated PLA maintains its biodegradability. Weight loss of the PLA films at each time point can be seen in Fig. 4a. When comparing the results of each coated film with uncoated PLA, no significant difference was found at any time point. At 168 h, coated and uncoated PLA films lost 80 to 88% of their initial weight. pH measurement of the enzyme solution after each time point was performed to confirm the degradation process, as lactic acid (a degradation product) is expected to be produced
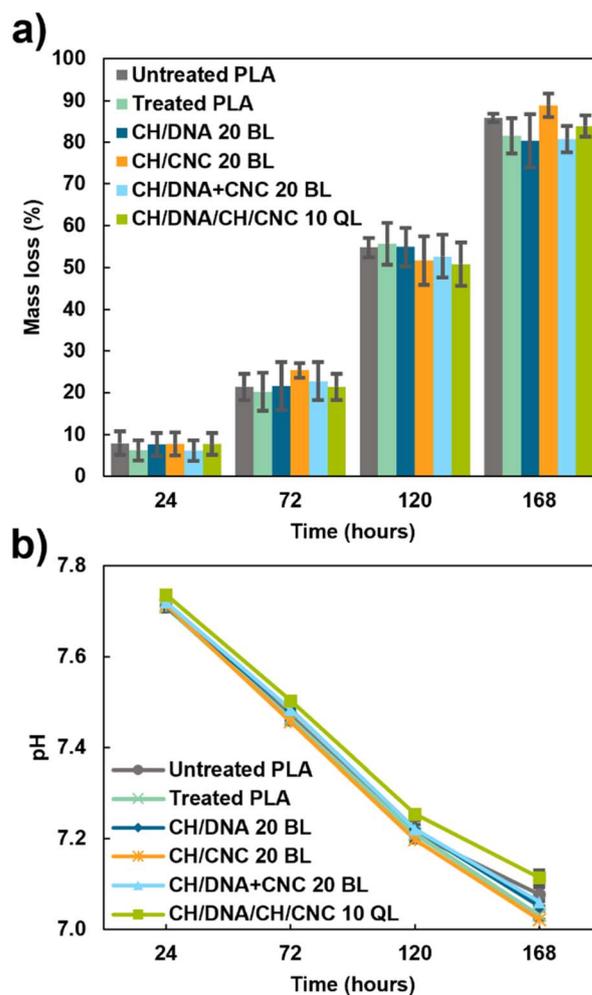
during the hydrolysis. The initial pH of 8 was decreased to nearly 7 after 168 h of treatment. No significant difference was observed between coated and uncoated (or plasma treated and untreated) PLA films at any time point (Fig. 4b). These results confirm that the barrier coatings do not impede the biodegradability of the PLA substrate.

Sustainability and comparison with literature

This treatment fits within several of the principles of green chemistry.[35] The materials that make up the LbL coatings are biobased, inherently non-toxic, industrially available materials that can all be sourced from existing waste streams.[2,4,36] Chitosan is primarily obtained from shellfish waste and is already available on a large scale.[2] DNA can theoretically be extracted from any organism on Earth, and is commonly sourced from waste products of the fishing industry (the source for the DNA used in this work).[36–38] Cellulose nanocrystals can also be extracted from waste biomass and are available on an industrial scale.[4,17,18] Unlike inorganic additives such as nanoclays, CNCs

require relatively low energy consumption to produce, are considered a renewable resource, and are biodegradable.[4] The film deposition procedure requires no solvent other than water and is performed under ambient conditions with no need for vacuum or high temperatures. Furthermore, the LbL coatings are shown to have little to no impact on the biodegradability of the PLA substrate. This eliminates the need for recycling or incineration at the end of life, which are both complex and expensive.[5]

In order to compare the barrier results with other biobased barrier coatings in the literature, the relative barrier improvement was quantified as the Barrier Improvement Factor (BIF), which is defined as the oxygen permeability of the uncoated substrate divided by the oxygen permeability of the coated substrate.[39] Relative film thickness was defined as the ratio of the coating thickness to the thickness of the substrate. Compared to a previously reported work on a CH/DNA oxygen barrier coating, this work provides a 10× increase in BIF at low humidity and a 3× increase at high humidity at a fraction of the thickness.[16] Compared to this and other fully biobased gas barrier coatings,[14,16,40–45] the present work offers a significant improvement in oxygen barrier at a very low thickness. As shown in Fig. 5a, the relative barrier improvement, expressed in terms of BIF, ranges from 6 to 30 for the barriers reported in this work, at a relative thickness of 0.002 or less. This is a substantial improvement to other biobased barrier films, which only achieve similar BIF values at much higher relative thicknesses.

Other works in the literature report oxygen permeability values for the barrier coating only, decoupled from the substrate. When comparing these values, it can again be observed that the treatments reported in this work offer considerable improvements to current biobased oxygen barriers (Fig. 5b). The films detailed in this work exhibit some of the lowest oxygen permeability values reported for fully biobased films, at a significantly lower thickness than other coatings. This work represents a significant step forward for biobased gas barrier technology.

Conclusions

A fully biobased and biodegradable oxygen barrier coating was developed for a poly(lactic acid) substrate to improve the oxygen transmission rate by 30× at low humidity and 12× at high humidity. The coating exhibits among the best oxygen permeability values reported for biobased barrier coatings at nanometer thickness. It was observed that at low relative humidity, films containing cellulose nanocrystals exhibit lower oxygen permeabilities due to the formation of a tortuous pathway for oxygen molecules. At high humidities, cellulose nanocrystals are detrimental due to their extreme water sensitivity. The barrier technology and deposition process fulfill the principles of green chemistry and represent a significant improvement in sustainable barrier film technology.

Data availability

The data supporting this article have been included as part of the ESI.†

Author contributions

Sarah G. Fisher: conceptualization, investigation, formal analysis, validation, writing – original draft, writing – review & editing, visualization. Armagan Amanipour: methodology, investigation. Maya D. Montemayor: investigation. Ethan T. Iverson: investigation. Edward Chang: investigation. Alexandra V. Moran: investigation. Reza Ovissipour: supervision, resources. Jaime C. Grunlan: supervision, resources, writing – review & editing. All authors have given approval to the final version of the manuscript.

Conflicts of interest

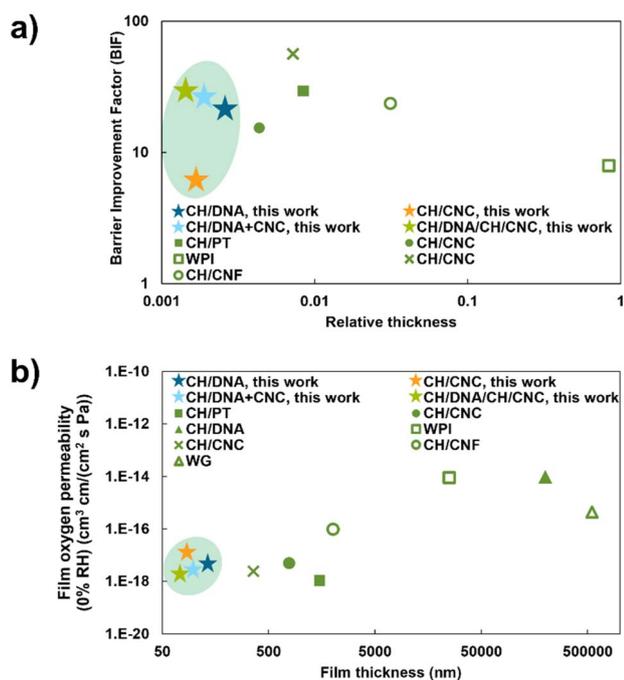There are no conflicts to declare.

Acknowledgements

Fig. 5 (a) BIF as a function of relative thickness and (b) oxygen permeability as a function of thickness of biobased barrier films at 0% RH. CH = chitosan; PT = pectin; CNC = cellulose nanocrystals; WPI = whey protein isolate; CNF = cellulose nanofibers; WG = wheat gluten.[14,16,40–45]

material are those of the author(s) and do not necessarily reflect the views of the National Science Foundation.

References

1 X. Zhao, K. Cornish and Y. Vodovotz, *Environ. Sci. Technol.*, 2020, **54**, 4712–4732.

2 J. R. Westlake, M. W. Tran, Y. Jiang, X. Zhang, A. D. Burrows and M. Xie, *Sustainable Food Technol.*, 2023, **1**, 50–72.

3 M. Asgher, S. A. Qamar, M. Bilal and H. M. N. Iqbal, *Food Res. Int.*, 2020, **137**, 109625.

4 J. Jacob, N. Linson, R. Mavelil-Sam, H. J. Maria, L. A. Pothan, S. Thomas, S. Kabdrakhmanova and D. Laroze, *Cellulose*, 2024, **31**, 5997–6042.

5 N. F. Zaaba and M. Jaafar, *Polym. Eng. Sci.*, 2020, **60**, 2061–2075.

6 P. Cazón and M. Vázquez, *Environ. Chem. Lett.*, 2020, **18**, 257–267.

7 Y. Zhao, C. Huang, R. Bei, H. Su and S. Wang, *J. Coat. Technol. Res.*, 2018, **15**, 505–514.

8 S. Singha and M. S. Hedenqvist, *Polymers*, 2020, **12**(5), 1095.

9 J.-W. Rhim, *Food Res. Int.*, 2013, **51**, 714–722.

10 *Multilayer Thin Films*, ed. G. Decher and J. B. Schlenoff, Wiley-VCH Verlag & Co., Weinheim, 2nd edn, 2012.

11 M. A. Priolo, K. M. Holder, T. Guin and J. C. Grunlan, *Macromol. Rapid Commun.*, 2015, **36**, 866–879.

12 G. Laufer, C. Kirkland, A. A. Cain and J. C. Grunlan, *ACS Appl. Mater. Interfaces*, 2012, **4**, 1643–1649.

13 Z. Yu, Y. Ji and J. C. Meredith, *ACS Appl. Polym. Mater.*, 2022, **4**, 7182–7190.

14 F. Li, P. Biagioni, M. Finazzi, S. Tavazzi and L. Piergiovanni, *Carbohydr. Polym.*, 2013, **92**, 2128–2134.

15 R. Rampazzo, D. Alkan, S. Gazzotti, M. A. Ortenzi, G. Piva and L. Piergiovanni, *Packag. Technol. Sci.*, 2017, **30**, 645–661.

16 L. Valle, L. Maddalena, G. Damonte, F. Carosio, A. Pellis and O. Monticelli, *Colloids Surf. B Biointerfaces*, 2024, **236**, 113806.

17 J. George and S. Sabapathi, *Nanotechnol. Sci. Appl.*, 2015, **8**, 45–54.

18 G. Fotie, R. Rampazzo, M. A. Ortenzi, S. Checchia, D. Fessas and L. Piergiovanni, *Polymers*, 2017, **9**, 415.

19 K. Halász, Y. Hosakun and L. Csóka, *Int. J. Polym. Sci.*, 2015, **2015**, e954290.

20 C. Wang, M. J. Park, H. Yu, H. Matsuyama, E. Drioli and H. K. Shon, *J. Membr. Sci.*, 2022, **661**, 120926.

21 J. B. Schlenoff and S. T. Dubas, *Macromolecules*, 2001, **34**, 592–598.

22 P. Podsiadlo, M. Michel, J. Lee, E. Verploegen, N. Wong Shi Kam, V. Ball, J. Lee, Y. Qi, A. J. Hart, P. T. Hammond and N. A. Kotov, *Nano Lett.*, 2008, **8**, 1762–1770.

23 E. T. Iverson, H.-C. Chiang, S. G. Fisher, H. Legendre, K. Schmieg, E. Chang and J. C. Grunlan, *Macromol. Mater. Eng.*, 2024, **309**, 2300407.

24 S. Qin, Y. Song, M. E. Floto and J. C. Grunlan, *ACS Appl. Mater. Interfaces*, 2017, **9**, 7903–7907.

25 F. Gao, *Mater. Today*, 2004, **7**, 50–55.

26 E. L. Cussler, S. E. Hughes, W. J. Ward and R. Aris, *J. Membr. Sci.*, 1988, **38**, 161–174.

27 D. Roilo, P. N. Patil, R. S. Brusa, A. Miotello, S. Aghion, R. Ferragut and R. Checchetto, *Polymer*, 2017, **121**, 17–25.

28 M. A. Priolo, K. M. Holder, S. M. Greenlee, B. E. Stevens and J. C. Grunlan, *Chem. Mater.*, 2013, **25**, 1649–1655.

29 R. J. Ashley, in *Polymer Permeability*, ed. J. Comyn, Springer Netherlands, Dordrecht, 1985, pp. 269–308.

30 D. Reishofer, R. Resel, J. Sattelkow, W. J. Fischer, K. Niegelhell, T. Mohan, K. S. Kleinschek, H. Amenitsch, H. Plank, T. Tammelin, E. Kontturi and S. Spirk, *Biomacromolecules*, 2022, **23**, 1148–1157.

31 R. Auras, B. Harte and S. Selke, *J. Appl. Polym. Sci.*, 2004, **92**, 1790–1803.

32 R. J. Hernandez, in *Water in Foods*, ed. P. Fito, A. Mulet and B. McKenna, Pergamon, Amsterdam, 1994, pp. 495–507.

33 M. Bartel, H. Remde, A. Bohn and J. Ganster, *J. Appl. Polym. Sci.*, 2017, **134**(5), DOI: **10.1002/app.44424**.

34 B. J. Ryan and K. M. Poduska, *Am. J. Phys.*, 2008, **76**, 1074–1077.

35 P. T. Anastas and J. C. Warner, *Green Chemistry: Theory and Practice*, Oxford University Press, 1998.

36 Y. Takahashi, K. Kondo, A. Miyaji, Y. Watanabe, Q. Fan, T. Honma and K. Tanaka, *PLoS One*, 2014, **9**, e114858.

37 Y. Ji, T. Kim, D. Han and J. B. Lee, *ACS Mater. Lett.*, 2024, 1277–1287.

38 J. Alongi, R. A. Carletto, A. D. Blasio, F. Carosio, F. Bosco and G. Malucelli, *J. Mater. Chem. A*, 2013, **1**, 4779–4785.

39 K. VaÅ¡ko, K. Noller, M. Mikula, S. Amberg-Schwab and U. Weber, *Open Phys.*, 2009, **7**, 371–378.

40 H.-C. Chiang, B. Eberle, D. Carlton, T. J. Kolibaba and J. C. Grunlan, *ACS Food Sci. Technol.*, 2021, **1**, 495–499.

41 O. Weizman, A. Dotan, Y. Nir and A. Ophir, *Polym. Adv. Technol.*, 2017, **28**, 261–270.

42 M. Guivier, G. Almeida, S. Domenek and C. Chevigny, *Carbohydr. Polym.*, 2023, **312**, 120761.

43 V. T. Tuyet Thuy, L. Tan Hao, H. Jeon, J. Mo Koo, J. Park, E. Seong Lee, S. Yeon Hwang, S. Choi, J. Park and D. X. Oh, *Green Chem.*, 2021, **23**, 2658–2667.

44 H. Kjellgren, M. Gällstedt, G. Engström and L. Järnström, *Carbohydr. Polym.*, 2006, **65**, 453–460.

45 M. Gällstedt, A. Brottman and M. S. Hedenqvist, *Packag. Technol. Sci.*, 2005, **18**, 161–170.